



Dalton
Transactions

**From $\text{Ln}_2\text{O}_2\text{S}$ to $\text{Ln}_{10}\text{OS}_{14}$: Exploring the sulphur spectrum
of trivalent lanthanoid oxysulphides**

Journal:	<i>Dalton Transactions</i>
Manuscript ID	DT-FRO-01-2024-000294.R1
Article Type:	Frontier
Date Submitted by the Author:	07-Mar-2024
Complete List of Authors:	Wuille Bille, Brian; Max-Planck-Institute for Chemical Energy Conversion, Chemistry Velázquez, Jesús; University of California, Davis, Chemistry and Chemical Engineering

SCHOLARONE™
Manuscripts

ARTICLE

From $\text{Ln}_2\text{O}_2\text{S}$ to $\text{Ln}_{10}\text{OS}_{14}$: Exploring the sulphur spectrum of trivalent lanthanoid oxysulphides

Brian A. Wuille Bille,^{a,b} and Jesús M. Velázquez^{*b}

Received 00th January 20xx,
Accepted 00th January 20xx

DOI: 10.1039/x0xx00000x

While $\text{Ln}_2\text{O}_2\text{S}$ oxysulphides have increasingly gained attention for their structural and optoelectronic properties, an expansive compositional space lies beyond as the sulphur-to-oxygen ratio increases. In these oxysulphides, the compounded effect of the 4f states manifold in the lanthanoid ions and the changing bonding and environment symmetry enables the tuning of their electronic structure and photophysical properties. Their challenging syntheses have rendered these materials largely unexplored, but recent efforts have been made to bridge the knowledge gap. In this article we present some of the structural characteristics and photophysical properties of the lanthanoid oxysulphide spectrum $\text{Ln}_x\text{O}_y\text{S}_z$.

Introduction

Lanthanoid oxysulphides, of general formula $\text{Ln}_x\text{O}_y\text{S}_z$, comprehend a large class of materials with differing sulphur-to-oxygen ratios. Since the structure of an oxysulphide was first elucidated in 1947,¹ these materials have been extensively studied due to their multitude of technological applications as colour-tunable phosphors,² sulphur-tolerant³ catalyst supports for the water gas shift reaction,⁴ in magnetism,⁵ and luminescence thermal sensing.⁶⁻⁹ While the compositional space is large, $\text{Ln}_2\text{O}_2\text{S}$ has been the most widely explored stoichiometry,¹⁰⁻¹² and considerably less information is available on its remaining congeners.^{13, 14} Only recently was the $\text{Ln}_2\text{O}_2\text{S}_2$ crystal structure understood owing to the disorder present in disulphide layer.¹⁵ Similarly, little is known on the mixed lanthanoid and solid solution ranges in the $\text{Ln}_{10}\text{S}_{15-x}\text{O}_x$ system and the impact that the substitution of oxygen has on its crystal and electronic structures. Furthermore, for all compositions besides $\text{Ln}_2\text{O}_2\text{S}$, their photophysics are largely unknown.

In this article, we introduce the compositional spectrum of lanthanoid oxysulphides, summarize some of their salient properties and indicate where knowledge gaps reside. We emphasize on the large opportunity for contributions to expand our limited knowledge of this exciting class of lanthanoid mixed anion materials.

Structural Versatility

From $\text{Ln}_2\text{O}_2\text{S}$ to $\text{Ln}_{10}\text{OS}_{14}$

In the large majority of lanthanoid oxysulphides, the cations adopt their most common +3 oxidation state, while the anions attain their -2 oxidation state, with the exception of $\text{Ln}_2\text{O}_2\text{S}_2$. Furthermore, due to their large ionic radius, the lanthanoid ions have high coordination numbers, typically between 7 - 8. In $\text{Ln}_2\text{O}_2\text{S}$, which crystallizes in the $P-3m1$ space group, the Ln^{3+} ions are coordinated by three S^{2-} and four O^{2-} in a capped trigonal antiprism along the c-axis, which results in a local C_{3v} symmetry (**Figure 1a**). The oxydisulphides, Ln_2OS_2 , of space group $P21/c$, demonstrate more asymmetric 7-fold coordination environments, in its two distinct crystallographic sites (**Figure 1c**). At the end of the spectrum, the highest sulphur content oxysulphide, $\text{Ln}_{10}\text{OS}_{14}$ exhibits a tetragonal unit cell and multitude of 8-fold coordinated crystallographic sites. Its atomic structure can be described as O-centred tetrahedra $[\text{OLn}_4]^{10+}$ surrounded by a "sea" of lanthanoid sulphide (**Figure 1d**).¹⁶ Departing from the rest of the members, $\text{Ln}_2\text{O}_2\text{S}_2$ possesses a layered structured, in which fluorite-type $[\text{Ln}_2\text{O}_2]^{2+}$ are separated by $(\text{S}_2)^{2-}$ dimers (**Figure 1b**). Interestingly, the degree of disorder in the disulphide layer determines the specific crystal group (Cmnc or $I4/mmm$) as well as its topochemical reactivity.¹⁵

Cation substitution

Owing to the similarities in the lanthanoids' ionic radii, each oxysulphide crystal structure affords a large compositional space. Through the combination of different lanthanoid ions, a great variety of properties can be tailored. One such strategy

^a Present address: Department of Inorganic Spectroscopy, Max Planck Institute for Chemical Energy Conversion, Mülheim an der Ruhr, 45470, Germany

^b Department of Chemistry, University of California, Davis, 95616, United States of America

E-mail: jevelazquez@ucdavis.edu

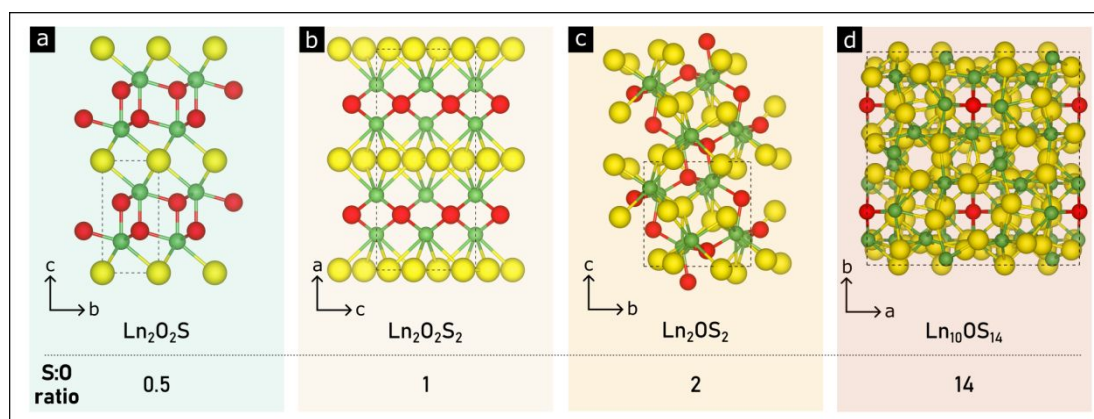


Figure 1. Crystal structures of the lanthanoid oxysulphides and their S:O ratio. Unit cells are designated with dashed lines. The green, red, and yellow circles represent Ln^{3+} , O^{2-} , and S^{2-} , respectively, represented with their atomic radii. Created with VESTA.⁴⁵

involves doping, or the incorporation of small quantities, into the lattice of the host material. Well beyond the oxysulphides, doping of rare earth ions, most commonly of the highly luminescent Eu, Er, Tb, and Yb, has been extensively used for the synthesis of enhanced luminescent semiconductors, nanoscrolls,¹⁷ and in upconverted emission.^{7, 18} Oxysulphides can similarly act as hosts, with the benefit of high chemical stability, general low-toxicity and high thermal sensitivity, characteristics that are especially important in their application in biological media and thermometry. Alternatively, binary, ternary and multinary lanthanoid oxysulphides can be synthesized. If the ionic radius tolerance is satisfied for the specific crystal structure, then more dramatic effects on its properties can be elicited by the combination of rare earth ions, like those observed in the band gap energies in a series of bimetallic $(\text{Ce,Gd})_2\text{O}_2\text{S}$.¹² Therein, the band gap decreased progressively with Ce content, and so did its magnetic moment given the decrease in the number of 4f electrons of the lanthanoid ion (from 4f⁷ in Gd^{3+} , to 4f¹ in Ce^{3+}).⁵ In addition, if these bimetallic oxysulphides are doped with a tertiary lanthanoid, even a finer modulation of the material properties can be achieved. Such is the example of $(\text{Lu,Gd})_2\text{O}_2\text{S}:\text{Tb}^{3+}$ and $(\text{Y,Gd})_2\text{O}_2\text{S}:\text{Tb}^{3+}$ systems, in which Lu and Y influence the energy transfer with the dopant ions, resulting in greater colour change as a function of solid solution composition in the latter.¹⁹ These strategies have paved the way for the exciting recent investigations into high-entropy oxysulphides that may unlock new reactivity and optoelectronics in this family of materials.^{20, 21}

Photophysics

Much like in oxynitrides and oxyhalides, the presence of mixed anions in oxysulphides enables the expression/enhancement of properties absent in the mono-anionic counterparts.^{22, 23} In particular, in terms of their photophysical properties, oxysulphides generally exhibit narrower bandgaps than their corresponding oxides. While structural differences certainly play a role in their band structures, in lanthanoid oxysulphides, valence band maxima are mostly of anion character, whereas the conduction band minima are dominated by lanthanoid 5d

states (or transition metal d-states in multinary oxysulphides). Thus, the higher energy of the frontier sulphur orbitals leads to a rise in the valence band maximum, resulting in a decrease in the band gap energy. As a consequence, most lanthanoid oxysulphides are semiconductors with colours in the visible range of the electromagnetic spectrum (**Figure 2**).

At a first glance, both in $\text{Ln}_2\text{O}_2\text{S}$ and $\text{Ln}_{10}\text{OS}_{14}$, there seems to be no clear trend in the measured optical band gap energies as a function of lanthanoid identity (**Figure 2b** and **c**). Although the 4f orbitals tend to be unaffected by their chemical environment, their electrons interact with electromagnetic radiation, and they do so in rather complex manners.²⁴ In fact, the degree of covalency between the Ln 5d and the ligand orbitals can indirectly perturb the energy and intensity of the sharp f-f transitions.²⁵ Computational treatment of these states remains a challenge, however, it has become clear that they must be explicitly included in order to arrive at more accurate and quantitative descriptions of the electronic energy levels of lanthanoids.^{26, 27} Indeed, from comparative studies in sesquioxides (Ln_2O_3) it was shown the non-monotonic periodicity in their band gap energies. La and Gd, have no f bands in the band gap energy region, and their transitions are dominated by $\text{O } 2p \rightarrow \text{Ln } 5d$ states; in the first lanthanoids (Ce, Pr, and Nd) the fundamental band gap arises from transitions of $\text{Ln } 4f \rightarrow \text{Ln } 5d$ character; lastly, in the later lanthanoids (Pm – Tm) the transition occurs between $\text{O } 2p \rightarrow \text{Ln } 4f$ states. Similar conclusions were derived from an X-ray spectroscopic study by Altman et al.,²⁸ and their proposed qualitative band diagram is reproduced in **Figure 3b**. These observed trends in the band gap energies in oxides were qualitatively followed in our study on $\text{Ln}_{10}\text{S}_{14}\text{O}$ (**Figure 3a**, bottom) with a significant sub-bandgap photocurrent detected. Although the cause may be a combination of structural defects and lanthanoid 4f states.¹⁴ Nevertheless, given that the substitution of O^{2-} anions for softer S^{2-} changes the chemical environment and symmetry of the lanthanoids' coordination sphere, it would be of great interest to expand on these computational and spectroscopic studies to the full spectrum of lanthanoid oxysulphides, and understand the degree of participation of the 4f orbitals in their electronic structures.

Thermodynamic stability and synthesizability

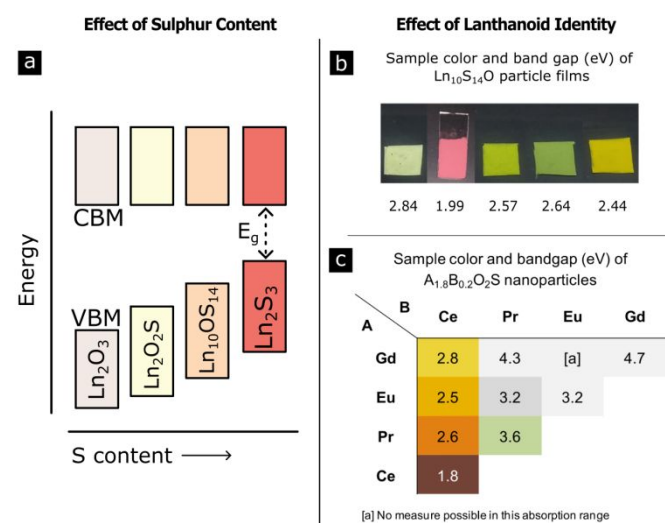


Figure 2. Photophysical properties of lanthanoid oxysulphides: a) Qualitative block diagram of the progressive valence band edge maximum (VBM) rise as a function of sulphur content; b) sample colour and band gap energy of $\text{Ln}_{10}\text{S}_{14}\text{O}$. Adapted with permission from ref. 14. Copyright 2022 by the American Chemical Society; c) sample colour and band gap energy of $\text{Ln}_2\text{O}_2\text{S}$. Adapted with permission from ref. 12. Copyright 2019 by the American Chemical Society.

Generally, the synthesis of sulphides and oxysulphides of the trivalent lanthanoid ions is energetically demanding. This is owing to the lower affinity that the hard acids, Ln^{3+} , have for S^{2-} – a soft base –, as opposed to the O^{2-} hard bases that are part of most starting materials. The milder synthetic conditions (temperatures of ca. 300°C) are suitable for colloidal nanoparticles of $\text{Ln}_2\text{O}_2\text{S}$, where high-boiling point coordinating solvents are used (like oleylamine and octadecene) in combination with the lanthanoid precursor and a sulphur source.²⁹ More recently thermal decomposition of single precursors, like thiocarbamates, have been used to great success.²⁰ However, in the solid state and for compositions with greater S:O ratio, temperatures between $600 - 1200^\circ\text{C}$ are required. Their syntheses involve a lanthanoid salt (e.g., oxides and sulphates) and elemental sulphur, if reacting in a closed vessel,^{15, 30, 31} or a sulphurizing agent (e.g. H_2S or CS_2) if the synthesis is carried under flow.^{10, 14}

$\text{Ln}_2\text{O}_2\text{S}$ oxysulphides have been synthesized for the majority of the lanthanoids. However, reports on the properties of the pure-phase heavier members (Tb–Lu) are rare.^{32–34} Similarly, the higher sulphur content members of the spectrum are mostly limited to the light rare earths (up to Gd). Despite their intriguing properties, there remains a large degree of uncertainty in the landscape of lanthanoid oxysulphides and the conditions required for their synthesis as the reports on the thermodynamics of these systems are scarce.^{35–37} Even the most complete account, by Vaughan and White,³⁷ is qualitative in many aspects and limited to only a few oxysulphides and their polymorphs (as seen in **Figure 4**). It is interesting to note how the region of existence of $\text{Ln}_{10}\text{OS}_{14}$ (the β polymorph) decreases along the lanthanoid series, matching our experimental observations, of more challenging pure-phase synthesis for the heavier lanthanoids. It is possible that the increasing ionicity of

the heavier lanthanoid trivalent cations renders bonding with

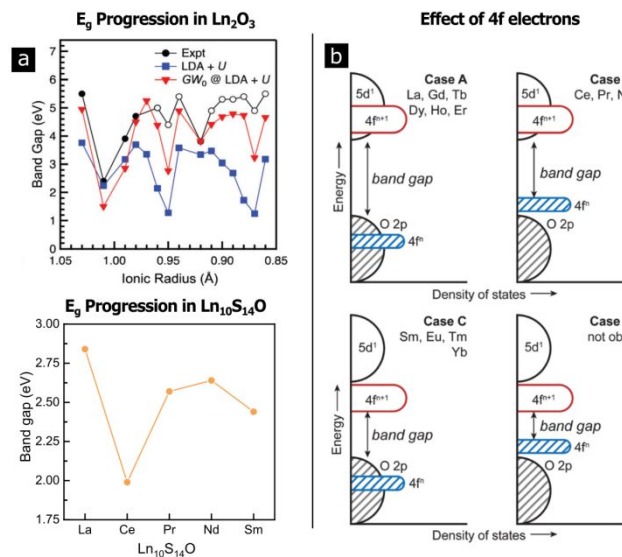


Figure 3. a) Top, band gap progression in Ln_2O_3 . Reproduced with permission from ref. 28. Copyright 2016 by the Royal Society of Chemistry. Bottom, band gap progression in $\text{Ln}_{10}\text{S}_{14}\text{O}$ as a function of lanthanoid cation; b) qualitative band diagram of Ln_2O_3 , reproduced with permission from ref. 28. Copyright 2016 by the Royal Society of Chemistry.

the softer sulphide ligand an even higher thermodynamic uphill battle. Hence the need for calorimetric studies which could provide solid foundational grounds to understand the stability and synthesizability of the known oxysulphide phases quantitatively, and a tool to expand the realm of compositions and polymorphism.

The case of cerium

Among the published literature, there is a remarkable distinct photophysical behaviour in the cerium oxysulphides in comparison with the rest of the rare earths,^{12, 14} likely originating from a unique electronic structure. Most lanthanoids can attain multiple oxidation states, beyond the common +3.^{38, 39} In cerium, the +4 oxidation state is particularly easily attainable, and has indeed been identified in its own series of oxysulphides.^{40–42} This proclivity to oxidation is responsible for stark colour changes in $\text{Ce}_2\text{O}_2\text{S}$ when exposed to O_2 .^{29, 43} However, it is yet unclear what determines the intrinsic distinction in cerium oxysulphides' optical properties with its congeners, in the absence of chemical changes. One such example is the similar band gap energies between $\text{Ce}_2\text{O}_2\text{S}$,²⁹ and $\text{Ce}_{10}\text{OS}_{14}$,¹⁴ irrespective of the sulphur content. It is possible that the absorption onset is dominated by the dipole allowed $4f \rightarrow 5d$ transitions in Ce^{3+} that appear as broad features centred at 500 nm.⁴⁴ Further spectroscopic measurements from the intermediate S-content oxysulphides would be instructive.

Conclusions and future outlook

Lanthanoid oxysulphides represent a large compositional space, where the sulphide content and lanthanoid identities can act as handles for targeted materials design. The entire sulphur

spectrum exhibits multiple interesting structural and opto-electronic properties, yet, most research has focused on the $\text{Ln}_2\text{O}_2\text{S}$ oxysulphides. While certainly deserving of further investigations, we believe that the higher-sulphur-containing

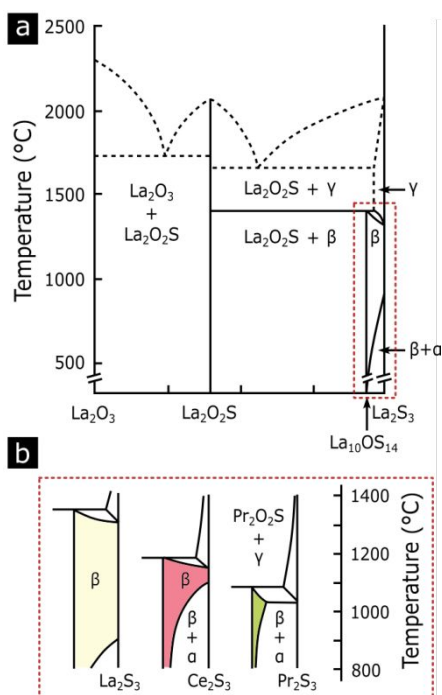


Figure 4. a) Compiled Ln-O-S phase diagram data for lanthanum; b) magnification of the high-S content portion of the phase diagram showing differences between La, Ce, and Pr. The coloured regions correspond to the $\text{Ln}_{10}\text{OS}_{14}$ polymorph, the β phase. Adapted with permission from ref. 37. Copyright 1987 by the Materials Research Society

oxysulphides, hold great untapped potential as multifunctional materials. This is because they combine the optical properties derived from the uniquely complex electronic structure of the lanthanoid ions with the tunability that a mixed-anion periodic solid can offer. As such, we envision that these oxysulphides could see wide ranging applications, from sulphur-involving batteries, in the case of $\text{Ln}_2\text{O}_2\text{S}_2$, for instance, to supports and local thermal sensors for catalysis under harsh environments. We hope this *Frontiers* article inspires further research into these exciting mixed-anion materials.

Conflicts of interest

There are no conflicts to declare

Acknowledgements

JMV thanks the University of California, Davis for start-up funding. JMV also acknowledges support from the Cottrell Scholars program supported by the Research Corporation for Science Advancement (RCSA 26780), as well as support from the National Science Foundation through the Faculty Early Career Development Program (DMR-2044403).

Notes and references

- J. J. Pitha, A. L. Smith and R. Ward, *Journal of the American Chemical Society*, 1947, **69**, 1870-1871.
- P. Liu, F. Wang, B. Yang and X. Chen, *Applied Physics A*, 2018, **125**.
- I. Valsamakis and M. Flytzani-Stephanopoulos, *Applied Catalysis B: Environmental*, 2011, DOI: 10.1016/j.apcatb.2011.05.037.
- S. Tan and D. Li, *ChemCatChem*, 2018, **10**, 550-558.
- C. Larquet, Y. Klein, D. Hrabovsky, A. Gauzzi, C. Sanchez and S. Carenco, *European Journal of Inorganic Chemistry*, 2019, DOI: 10.1002/ejic.201801466, 762-765.
- J. Jiao, Y. Liu, H. Wang, X. Yin, M. Xing, X. Luo and Y. Tian, *Journal of the American Ceramic Society*, 2020, **104**, 985-994.
- W. Zheng, B. Sun, Y. Li and R. Wang, *ACS Applied Nano Materials*, 2021, **4**, 3922-3931.
- Q. Zou, C. Marcelot, N. Ratel-Ramond, X. Yi, P. Roblin, F. Frenzel, U. Resch-Genger, A. Eftekhari, A. Bouchet, C. Coudret, M. Verelst, X. Chen, R. Mauricot and C. Roux, *ACS Nano*, 2022, **16**, 12107-12117.
- M. Jia, X. Chen, R. Sun, D. Wu, X. Li, Z. Shi, G. Chen and C. Shan, *Nano Research*, 2022, **16**, 2949-2967.
- E. I. Sal'nikova, Y. G. Denisenko and O. V. Andreev, *Inorganic Materials*, 2022, **58**, 516-524.
- L. Meyniel, C. Boissiere, N. Krins and S. Carenco, *Langmuir*, 2023, **39**, 728-738.
- C. Larquet, A.-M. Nguyen, E. Glais, L. Paulatto, C. Sassoey, M. Selmane, P. Lecante, C. Maheu, C. Geantet, L. Cardenas, C. Chanéac, A. Gauzzi, C. Sanchez and S. Carenco, *Chemistry of Materials*, 2019, **31**, 5014-5023.
- T. Schleid and F. Lissner, *Journal of the Less-Common Metals*, 1991, **175**, 309-319.
- B. A. Wuille Bille, A. C. Kundmann, F. E. Osterloh and J. M. Velázquez, *Chemistry of Materials*, 2022, **34**, 7553-7562.
- L. B. Mvélé, S. Sasaki, C. Latouche, P. Deniard, E. Janod, I. Braems, S. Jobic and L. Cario, *Inorg Chem*, 2023, **62**, 7264-7272.
- P. Besançon, *Journal of Solid State Chemistry*, 1973, **7**, 232-240.
- X. Ou, X. Qin, B. Huang, J. Zan, Q. Wu, Z. Hong, L. Xie, H. Bian, Z. Yi, X. Chen, Y. Wu, X. Song, J. Li, Q. Chen, H. Yang and X. Liu, *Nature*, 2021, **590**, 410-415.
- E. M. Chan, G. Han, J. D. Goldberg, D. J. Gargas, A. D. Ostrowski, P. J. Schuck, B. E. Cohen and D. J. Milliron, *Nano Lett*, 2012, **12**, 3839-3845.
- N. Pasberg, D. den Engelsen, G. R. Fern, P. G. Harris, T. G. Ireland and J. Silver, *Dalton Trans*, 2017, **46**, 7693-7707.
- B. Ward-O'Brien, E. J. Pickering, R. Ahumada-Lazo, C. Smith, X. L. Zhong, Y. Aboura, F. Alam, D. J. Binks, T. L. Burnett and D. J. Lewis, *J Am Chem Soc*, 2021, **143**, 21560-21566.
- B. Ward-O'Brien, P. D. McNaughtner, R. Cai, A. Chattopadhyay, J. M. Flitcroft, C. T. Smith, D. J. Binks, J. M. Skelton, S. J. Haigh and D. J. Lewis, *Nano Lett*, 2022, **22**, 8045-8051.
- M. Yang, J. Oró-Solé, J. A. Rodgers, A. B. Jorge, A. Fuertes and J. P. Attfield, *Nature Chemistry*, 2011, **3**, 47-52.
- X. Chen and K. M. Ok, *Chem Sci*, 2022, **13**, 3942-3956.
- J. L. Mason, H. Harb, J. E. Topolski, H. P. Hratchian and C. C. Jarrold, *Acc Chem Res*, 2019, **52**, 3265-3273.
- B. S. Zanella, S. B. Jones, H. S. Lee and R. D. Hancock, *Inorg Chem*, 2022, **61**, 4627-4638.
- M. Mikami and S. Nakamura, *Journal of Alloys and Compounds*, 2006, **408-412**, 687-692.
- R. Gillen, S. J. Clark and J. Robertson, *Physical Review B*, 2013, **87**.
- A. B. Altman, J. I. Pacold, J. Wang, W. W. Lukens and S. G. Minasian, *Dalton Trans*, 2016, **45**, 9948-9961.
- C. Larquet, A. M. Nguyen, M. Avila-Gutierrez, L. Tinat, B. Lassalle-

- Kaiser, J. J. Gallet, F. Bournel, A. Gauzzi, C. Sanchez and S. Carencio, *Inorg Chem*, 2017, **56**, 14227-14236.
30. F. Lissner and T. Schleid, *Z. Naturforsch.*, 1992, **47b**, 1614-1620.
31. T. Schleid and F. A. Weber, *Zeitschrift für Kristallographie*, 1998, **213**.
32. Y. Abbas, J. Rossat-Mignod, F. Tcheu and G. Quezel, *Physica 86-88B*, 1977, 115-117.
33. X.-F. Zhang, H.-H. Zou, L.-W. Ding, X.-X. Deng, J.-J. Zheng, H.-F. Liu, Z.-M. Ye, S. Zhong, Z.-Y. Du, J. Zhang and C.-T. He, *Cell Reports Physical Science*, 2023, **4**.
34. P. Chen, B. Peng, Z. Liu, J. Liu, D. Li, Z. Li, X. Xu, H. Wang, X. Zhou and T. Zhai, *Journal of the American Chemical Society*, 2024, DOI: 10.1021/jacs.3c13267.
35. R. J. Fruehan, *Metallurgical Transactions B* 1979, **10B**, 143-148.
36. M. Leskelä, *Thermochimica Acta*, 1985, **92**, 739-742.
37. C. M. Vaughan and W. B. White, *Mat. Res. Soc. Symp. Proc.*, 1987, **97**, 397-402.
38. M. Tricoire, N. Mahieu, T. Simler and G. Nocton, *Chemistry - A European Journal*, 2021, **27**, 6860-6879.
39. T. P. Gomba, A. Ramanathan, N. T. Rice and H. S. La Pierre, *Dalton Trans*, 2020, **49**, 15945-15987.
40. P. J. Dugué, D. Carré and M. Guittard, *Acta Cryst.*, 1978, **B34**, 3564-3568.
41. P. J. Dugué, D. Carré and M. Guittard, *Acta Cryst.*, 1979, **B35**, 1550-1554.
42. W. Wichelhaus, *Angewandte Chemie International Edition*, 1978, **17**, 451-452.
43. C. Sourisseau, R. Cavagnat, R. Mauricot, F. Boucher and M. Evain, *Journal of Raman Spectroscopy*, 1997, **28**, 965-971.
44. J. Xu, S. Tanabe, A. D. Sontakke and J. Ueda, *Applied Physics Letters*, 2015, **107**, 081903.
45. K. Momma and F. Izumi, *Journal of Applied Crystallography*, 2008, **41**, 653-658.